Eur. Phys. J. A **6**, 251–255 (1999)

THE EUROPEAN PHYSICAL JOURNAL A

Favoured superdeformed states in ^{89}Tc

B. Cederwall[1], T. Bäck[1], R. Wyss[1], A. Johnson[1], J. Cederkäll[1,a], M. Devlin[2], J. Elson[2], D.R. LaFosse[2,b], F. Lerma[2], D.G. Sarantites[2], R.M. Clark[3], P. Fallon[3], I.Y. Lee[3], A.O. Macchiavelli[3], R.W. Macleod[3]

[1] Department of Physics, Royal Institute of Technology, 104 05 Stockholm, Sweden
[2] Chemistry Department, Washington University, St. Louis, MO 63130, USA
[3] Nuclear Science Division, Lawrence Berkeley National Laboratory, Berkeley, CA, 94720 USA

Received: 6 July 1999
Communicated by B. Herskind

Abstract. A superdeformed band consisting of a cascade of ten γ-ray transitions has been identified and assigned to the nucleus ^{89}Tc, close to the proton dripline. The quadrupole moment of the band ($Q_t = 6.7^{+3.0}_{-2.3}$ *eb*, as measured by the Residual Doppler Shift Method) as well as a large dynamic moment of inertia point to a highly elongated shape. With a relative population of approximately 15% of the γ-ray flux in the ^{89}Tc exit channel, the band is among the most intense superdeformed bands observed to date.

PACS. 21.10.Re Collective levels – 21.60.Cs Shell model – 23.20.Lv Gamma transitions and level energies – 27.50.+e $59 \leq A \leq 89$

Since the observation of the first high-spin superdeformed (SD) band in ^{152}Dy [1], SD shapes have been intensively studied in nuclei in the mass A∼80, A∼130, ∼150 and ∼190 regions [2–4]. Recently SD bands were discovered in the nuclei ^{60,62}Zn [5,6], possibly indicating yet another region of SD nuclei around mass A=60. Despite relatively long-standing theoretical predictions of the existence of a SD shell gap in A ∼ 80 nuclei [7–9] it was not until a few years ago that the first experimental observation of a SD band in ^{83}Sr was made by Baktash et al. [10]. The delay in experimental confirmation of the theoretical predictions is explained by the large difficulties associated with the detection of these typically very weak cascades of ∼ 1 - 3 MeV gamma rays, which can only be produced in rather unfavourable fusion-evaporation reactions with large reaction channel fragmentation. The combination of the latest generation of large γ-ray detector arrays [15,11] with ancillary charged particle detector systems [16] has been the key to the ongoing experimental success in unraveling the SD A∼80 mass region as well as the discovery of SD bands in ^{60,62}Zn.

In this article we report the observation of a SD band in ^{89}Tc. Together with the recent discoveries of SD bands in the N=46 isotones ^{87}Nb [12], ^{86}Zr [13] and ^{88}Mo [14] the A∼80 mass region of SD nuclei is now extended into A≈90. With an approximately 15% intensity relative to the total yield in the $2\alpha 2p$ channel leading to ^{89}Tc, this band is one of the most strongly populated SD bands ever observed (surpassed only by the recently observed SD band in ^{60}Zn [5] for which relative intensities of 34% and 60% were reported for two different experiments, respectively). The extracted lifetime information for the band indicates a quadrupole deformation which is at the high end of those observed for the A≈80 SD structures, similar to the A∼150 SD nuclei.

Excited states in ^{89}Tc were produced at the 88-Inch Cyclotron of Lawrence Berkeley National Laboratory using the ^{58}Ni(^{40}Ca,2α1p) reaction at 185 MeV bombarding energy. The highly enriched (99.8%) ^{58}Ni foil of 0.38 mg/cm^2 thickness, was placed at an angle of 30° relative to the beam direction, resulting in an effective thickness of 0.44 mg/cm^2. Gamma rays emitted in the reactions were observed with the Gammasphere [15] Ge detector array, then consisting of 94 large escape-suppressed coaxial n-type Ge detectors. The Microball [16], a 4π charged particle detector array with 95 CsI(Tℓ) scintillation detector elements was used in conjunction with Gammasphere to detect evaporated charged particles (mainly protons and alpha particles). This enabled a high selectivity for specific exit channels out of the large ensemble of species produced in the reactions. The event trigger required coincidences between three or more escape-suppressed Ge detectors. A total of 2.4×10^9 raw events were collected, sorted off-line into various particle-gated E_γ–E_γ coincidence matrices and E_γ–E_γ–E_γ coincidence cubes, and analysed using the Radware data analysis package [17] and other software. The detection efficiency for a proton was about 70% and

[a] *Present address:* Physics Department, Yale University, New Haven, CT 06520-8124, USA
[b] *Present address:* Department of Physics and Astronomy, State University of New York at Stony Brook, Stony Brook, NY 11794, USA

for an alpha particle about 45% in this case. Therefore, the $2\alpha 1p$ gate contained considerable admixtures of the $2\alpha 2p$, $2\alpha 3p$ and $3\alpha 1p$ reaction channels which "leaked through" when an α particle or a proton escaped detection. In the data analysis these contaminations could be subtracted using the corresponding particle-gated matrices. The final $2\alpha 1p$-gated "unfolded" coincidence data contained 4×10^7 $\gamma\gamma$ pairs from the decay of ^{89}Tc. For the relatively light compound nucleus ^{98}Cd, evaporated particles, especially α particles, have a sizeable effect on the momentum vector of the recoiling residual nuclei. Using the high granularity, particle identification, and energy information from the Microball, this was corrected for, significantly reducing the otherwise problematic Doppler broadening of the γ rays belonging to the $2\alpha 1$p exit channel.

From the particle-gated coincidence data, a rotational band of ten (eleven) γ-ray transitions with energies between 1147 keV and 2459 keV (tentatively 2625 keV) was established and assigned to the nucleus ^{89}Tc. The spectrum shown in Fig. 1 was obtained by summing all two-fold gates on the in-band γ rays from the $2\alpha 1p$-gated three-fold and higher-fold γ-ray coincidence data. The intensity of this SD band could be estimated to approximately 15% relative to the intensity flowing through the low-lying yrast states of ^{89}Tc. However, despite this high relative intensity, discrete linking transitions from the decay out of the band have not been identified and consequently the absolute spins and excitation energies of the SD states could not be determined. The observed decay pattern of the band is therefore consistent with the predominantly statistical character of the decay out of SD bands in other regions. Some indications of a proton decay branch out of the band (leading to excited states in ^{88}Mo) are not conclusive and need further studies. In the present analysis, three SD bands have also been assigned to the neighbouring N=46 isotone ^{88}Mo [14]. The most intense SD band in ^{88}Mo is used for comparison below. We have also found evidence for two other weak γ-ray cascades with SD characteristics which we have tentatively assigned to ^{89}Tc but which need further experimental confirmation.

The conventional Doppler Shift Attenuation Method of measuring line shapes in a backed target is not feasible for the very fast SD γ-ray transitions. However, lifetimes can be estimated by a technique [18] based on the residual Doppler shifts from the slowing down of the recoiling nuclei in a thin target. Such a residual Doppler shift analysis is presented in Fig. 2. The average recoil velocity was determined from the Doppler shifts of γ rays emitted from low-lying states in ^{88}Mo and ^{89}Tc. Such states have sufficiently long lifetimes in order to predominantly decay after the recoiling nuclei have passed out of the target and have a well-defined velocity distribution, $\langle v_0 \rangle$. However, the superdeformed states have much shorter lifetimes and a much larger fraction of them decays while the recoiling nuclei are slowing down in the target. Consequently, the fast γ rays in the SD band have different, larger, Doppler shifts. The average fractional shifts $F(\tau) = \langle v\ (\tau) \rangle / \langle v_0 \rangle$ are plotted as open and filled squares for the SD transitions in ^{89}Tc and ^{88}Mo, respectively. As a comparison,

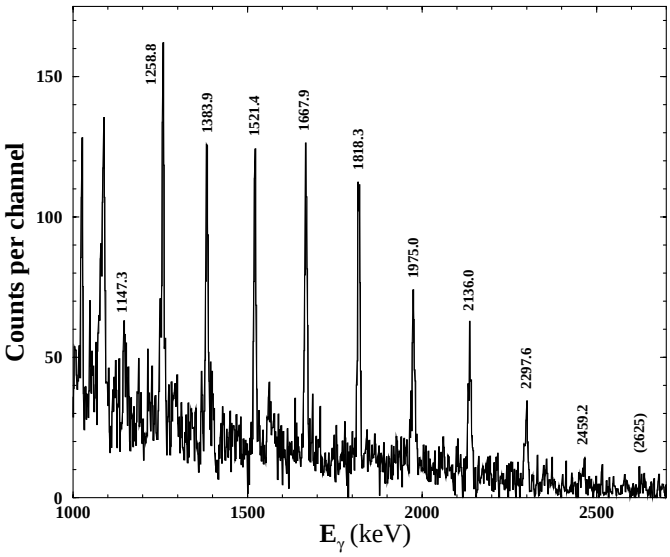

Fig. 1. Gamma-ray spectrum created by summing all combinations of double coincidence gates set on transitions belonging to the SD band in ^{89}Tc. Energies are labeled in keV and the energy dispersion is 2 keV per channel. The uncertainties in the energy determinations are estimated to vary between 0.5 and 1.0 keV. Relevant background contributions have been subtracted

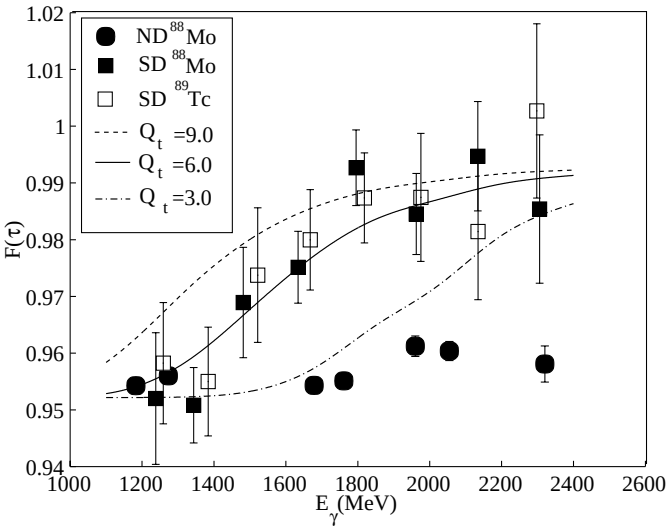

Fig. 2. Deduced $F(\tau)$ values as a function of γ-ray energy. The data points are extracted from the residual Doppler shifts of the γ-ray energies in the forward and backward detectors. Calculated $F(\tau)$ curves with different Q_t values are shown as lines. The data for ^{88}Mo are included for comparison since sufficiently intense low-lying yrast lines from the decay of this nucleus can be found in the SD spectral range

filled "circles" representing low-lying yrast transitions in ^{88}Mo (1273, 1679, 1761, 1960, 2055 and 2320 keV) are included. The slowing-down of the recoiling nuclei in the target was modeled using the electronic and nuclear stopping powers given by Ziegler *et al.* [19] and the velocity distribution of the recoiling nuclei was calculated as

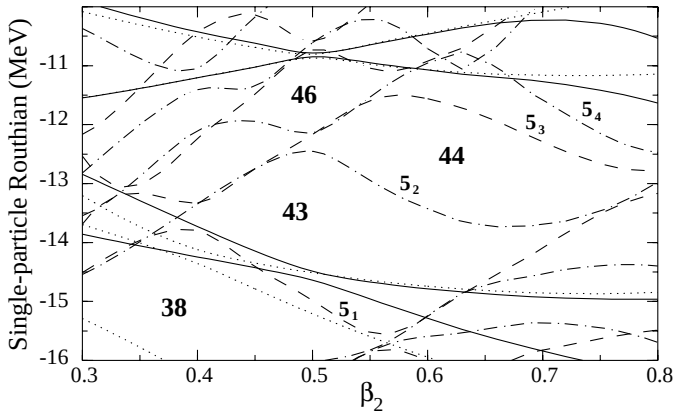

Fig. 3. Single-particle diagram of the deformed WS potential as a function of quadrupole deformation at a rotational frequency of $\hbar\omega$=0.8 MeV. The β_4 deformation was varied with β_2 corresponding to the minimum value of the total Routhian energy for each particle number. A triaxial deformation with $\gamma = 10^\circ$ was chosen, corresponding to the predicted shape of the yrast SD configuration in ^{89}Tc at $\hbar\omega$=0.8 MeV. The symbols for the different (π, α) configurations are: solid=$(+, \frac{1}{2})$, dotted=$(+, -\frac{1}{2})$, dash-dotted=$(-, \frac{1}{2})$, dashed=$(-, -\frac{1}{2})$. Particle numbers for the largest shell gaps and the $N = 5$ intruder orbits are indicated

a function of the decay time by integrating over the target material and averaging over three different reaction points in the target. Side feeding from rotational cascades with the same quadrupole moments was assumed according to the experimental feeding pattern. The experimental $F(\tau)$ values are compared with these calculations yielding a quadrupole moment $Q_t = 6.7^{+3.0}_{-2.3}$ eb for the SD band where the quoted error bar does not take into account any systematic uncertainties from the analysis. The deduced Q_t value corresponds to a quadrupole deformation of $\beta_2 \approx 0.6$, assuming an axially symmetric nuclear shape.

As pointed out above, the observed SD band in ^{89}Tc carries a relative intensity of about 15%. This can be compared to the intensity of the strongest band in the neighbouring nucleus ^{88}Mo which amounts to approximately 1% of the $2\alpha 2p$ channel. Relative SD band intensities on the order of 1% are representative of the A$\sim$ 80 region as well as other regions of SD nuclei. The strong population of the ^{89}Tc band is therefore clearly remarkable and demands an explanation. In order to shed light on this feature in particular and on the structure of A$\sim$90 SD nuclei in general we have performed cranked mean field calculations based on a Woods-Saxon potential [21, 20]. The pairing interaction was treated selfconsistently using both monopole and quadrupole components [22]. In order to avoid the spurious pairing-phase transition an approximate particle number projection using the Lipkin-Nogami approach [23,24] was performed. Excited quasiparticle configurations are blocked selfconsistently and the "routhian" energy in the rotating frame of reference was minimised with respect to the β_2, β_4 and γ deformation parameters for each configuration. More details concerning these extended total routhian surface (TRS) calculations can be found in [22]. The theoretically predicted 'doubly-magic' SD nucleus in the $A \approx 90$ region is the not yet observed nuclide $^{88}_{44}$Ru$_{44}$ (Fig. 3). The yrast SD configuration of this nucleus includes four particles in the $h_{11/2}$ ($\mathcal{N} = 5$) intruder orbitals (two protons and two neutrons), which we denote as $\pi 5^2 \nu 5^2$. Most of the SD nuclei observed up to now in this mass region can be assigned to the $\pi 5^1 \nu 5^2$ configuration. However, for the SD Sr-nuclei only one single $\mathcal{N} = 5$ neutron orbital and no $\mathcal{N} = 5$ proton orbitals are predicted to be occupied [25]. For Z$>$ 38 the $\mathcal{N} = 5$ proton orbital may become occupied as is seen in Fig. 3, showing the favoured Z=38, 43 and 44 gaps which separate the 5^0 from the 5^1, the 5^1 from the 5^2, and the 5^2 from the 5^3 proton configurations, respectively. The experimental observation of a very strongly populated SD band in ^{89}Tc with a large deformation is thus in accord with our theoretical calculations, which produce a large SD shell gap for $Z = 43$.

For the spherical states at low excitation energy in ^{89}Tc and neighbouring nuclei it is rather easy to build angular momentum. This is due to the fact that the valence protons and neutrons occupy states in the middle of the g$_{9/2}$ subshell. However, the valence space is very limited and the maximum spins for the $g^n_{9/2}$ configuration are $I = 24\hbar$ for ^{88}Ru and ^{88}Mo and $I = \frac{45}{2}\hbar$ for ^{89}Tc. Higher spin states are built up by means of particle hole excitations from the $f_{5/2}$ orbits into the $g_{7/2}$ subshell, across the spherical shell closure, and are hence costly in energy. This results in a steeply upsloping 'spherical' yrast line, once the $g_{9/2}$ pairs are broken (Fig. 4), a property common for many A$\approx$90 nuclei near N=Z. Hence the balance between the excitation energy of the SD well and the cost of exciting particles across the N,Z = 50 spherical shell closure determines when and if SD states become yrast. From a theoretical stand point, Fig. 4 explains at least qualitatively the very strong population of the observed SD band in ^{89}Tc. The excitation energy relative to the low-lying spherical states of the yrast SD bands in ^{88}Mo and ^{89}Tc are about 8.5 MeV and 6.5 MeV at $I = 20\,\hbar$, respectively. Therefore it is consistent with the calculations that we find a stronger population of the SD states in ^{89}Tc than in ^{88}Mo. For the "doubly magic" SD nucleus ^{88}Ru the SD states are predicted to be 5.5 MeV excited above the yrast line at the same angular momentum, which is not so different from the case in ^{89}Tc. In ^{89}Tc the calculated yrast line of the low-lying "spherical" states exhibits a steep rise as a function of angular momentum starting at $I \approx 25\hbar$. The energetically most favoured SD band is built on the $\pi 5^1 \nu 5^2$ configuration with deformation parameters ($\beta_2 = 0.52$, $\gamma = 10^\circ$) at $\hbar\omega = 0.8$ MeV. It is predicted to form the yrast line above $I = 28\,\hbar$. The predicted transition quadrupole moment of this structure is $Q_t \approx 5.6$ eb which is in agreement with our experimental data. For ^{88}Mo the yrast SD band is predicted to have the same intruder configuration whereas for ^{88}Ru the predicted SD intruder content is $\pi 5^2 \nu 5^2$. For both ^{88}Ru and ^{88}Mo the SD structures are predicted to become yrast at roughly the same angular momentum as for ^{89}Tc. However, the spherical single-particle states above $I = 28\,\hbar$

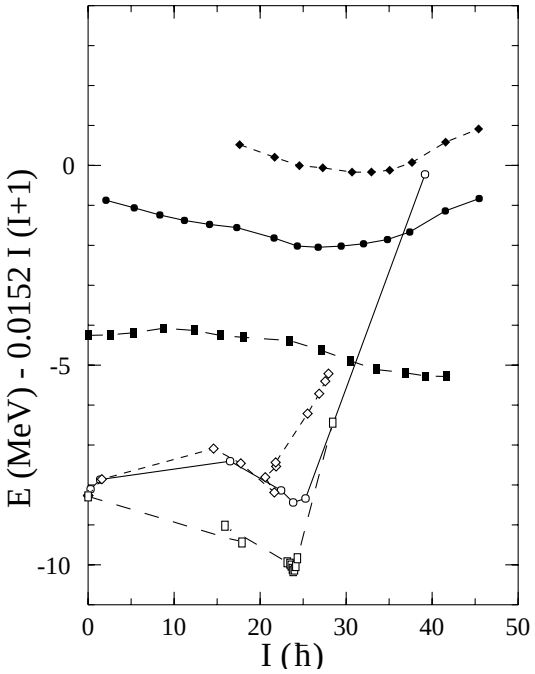

Fig. 4. Energy as a function of spin for the calculated spherical and SD configurations in ^{89}Tc (circles), ^{88}Ru (squares) and ^{88}Mo (diamonds). The energy is corrected with the energy of a rigid rotor with $\hbar^2/2\mathcal{J} = 0.0152$, where $\mathcal{J}$ is the moment of inertia. Open and filled symbols correspond to the yrast spherical configurations and the SD configurations, respectively

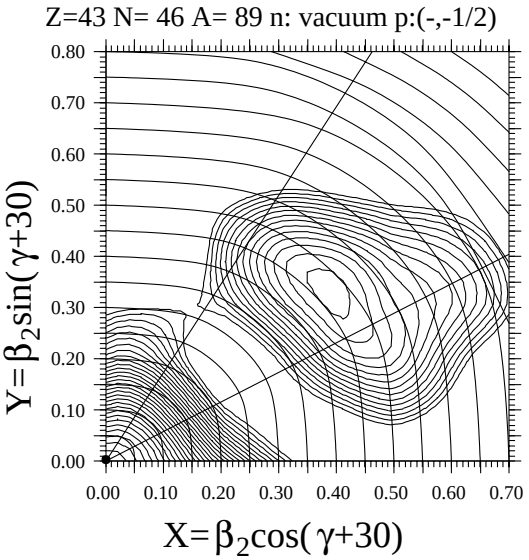

Fig. 5. Calculated total routhian surface at $\hbar\omega = 0.8$ MeV, based on the $(\pi, \alpha) = (-, -1/2)$ quasi-proton configuration. A well defined minimum is present around β_2=0.5. In addition, one may also see that an "enhanced SD" minimum is developing at $\beta_2 \approx$0.65

are too high in energy to be located in the present cranking approach.

The TRS for the $(\pi, \alpha) = (-, -\frac{1}{2})$ configuration in ^{89}Tc (which includes $\pi 5^1 \nu 5^2$) is shown in Fig. 5. In Fig. 6 the dynamic moment of inertia, $\mathcal{J}^{(2)}$, for the observed SD band is compared with the calculated values for the $\pi 5^1 \nu 5^2$ $(\pi, \alpha) = (-, -\frac{1}{2})$ configuration. The agreement between the experiment and the calculation is rather good, even though the bump in the theoretical $\mathcal{J}^{(2)}$ curve at $\hbar\omega \approx 1.3$ MeV is not observed. The increase in $\mathcal{J}^{(2)}$ in the calculations has its origin in a slight shape change towards larger triaxiality, and somewhat smaller β_2 and β_4 deformation $(\beta_2, \beta_4, \gamma)$: $(0.51, 0.02, 13°) \rightarrow (0.49, 0.01, 19°)$. This shape change is caused by a shift in the balance between the proton and neutron shell corrections with increasing rotational frequency. The neutron shell gap at N=46 is increasing with gamma deformation, which is one of the reasons for the triaxility of the SD bands in this mass region. At the same time, the proton shell correction is decreasing with angular momentum, due to the next N=5 proton intruder orbital approaching the Fermi surface. The change in angular momentum associated with this shape change is rather modest, of the order of 1-2$\hbar$. The discrepancy with respect to the experimental data points either to a somewhat weaker shell structure of the neutrons or that a coupling to the vibrational motion is washing out this mean-field effect. Many of the SD bands in this mass region are predicted to be quite soft with respect to gamma deformation, a property that is absent in other regions of SD nuclei. The observation of gamma-vibrations at SD shape would be a fingerprint of this softness and deserves further studies. Another interesting feature of the theoretical results is a pronounced "enhanced SD" minimum with $(\beta_2, \gamma) \approx (0.65, 0°)$ in the TRS above $\hbar\omega \approx 1$ MeV. This minimum is produced by occupying

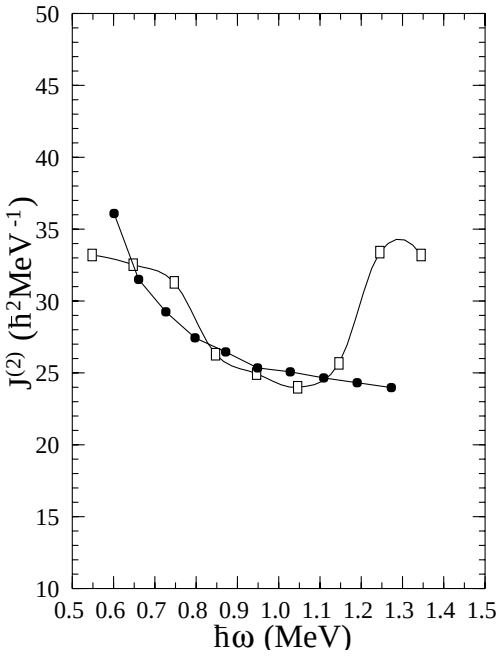

Fig. 6. Experimental dynamical moments of inertia $\mathcal{J}^{(2)}$ for the observed SD band (filled circles) compared to values from the cranked Strutinsky calculation (open boxes)

another pair of N=5 neutrons and is predicted to become yrast above $I \approx 40\hbar$. This may be an additional explanation for the strong population of the observed SD band, since the feeding of the band could be "funneled" through the continuum states in both the SD and enhanced SD wells.

According to our calculations $I^\pi = \frac{35}{2}^-$ may be assigned to the lowest observed SD state which would indicate that the band is observed up to tentatively $I = \frac{79}{2}\hbar$.

In summary we have identified a discrete-line superdeformed band in ^{89}Tc which consists of ten transitions and extends up to a tentative spin of $\frac{79}{2}\hbar$. The band properties are in fair agreement with cranked Woods-Saxon calculations. In particular, the very strong population of the observed SD band in ^{89}Tc can be explained by a combination of low relative excitation energy and a steeply upsloping spherical yrast line.

Thanks are due to Prof. H. Grawe for providing the targets. This work was supported in part by the Swedish Natural Science Research Council, and the U.S. Department of Energy; grant No. DE-FG05-88ER40406 (Washington University) and contract No. DE-AC03-76SF00098 (LBNL).

References

1. P.J. Twin *et al.*, Phys. Rev. Lett. **57**, 811 (1986)
2. P.J. Nolan and P.J. Twin, Ann. Rev. Nucl. Part. Sci. **38**, 533 (1988)
3. R.V.F. Janssens and T.L. Khoo, Ann. Rev. Nucl. Part. Sci. **41**, 321 (1991)
4. X.-L. Han and C.-L. Wu, At. Data Nucl. Data Tables **63**, 117 (1996)
5. C.E. Svensson *et al.*, Phys. Rev. Lett. **82**, 3400 (1999)
6. C.E. Svensson *et al.*, Phys. Rev. Lett. **79**, 1233 (1997)
7. I. Ragnarsson, S.G. Nilsson, and R.K. Sheline, Phys. Rep. **45**, 1 (1978)
8. W. Nazarewicz *et al.*, Nucl. Phys. **A435**, 397 (1985)
9. J. Dudek, W. Nazarewicz and N. Rowley, Phys. Rev. **C35**, 1489 (1987)
10. C. Baktash *et al.*, Phys. Rev. Lett. **74**, 1946 (1995)
11. J. Simpson, Z. Phys. **A358**, 139 (1997)
12. D.R. LaFosse *et al.*, Phys. Rev. Lett. **78**, 614 (1997)
13. D.G. Sarantites *et al.*, Phys. Rev. **C57**, R1 (1998)
14. T. Bäck *et al.*, submitted to Eur. Phys. J
15. Gammasphere Proposal, March 1988, LBL-PUB-5202; I.Y. Lee, Nucl. Phys. **A520**, 361 (1990)
16. D.G. Sarantites *et al.*, Nucl. Instr. and Meth. **A381**, 418 (1996)
17. D.C. Radford, Nucl. Inst. and Meth. **A361**, 297 (1995)
18. B. Cederwall *et al.*, Nucl. Inst. and Meth. **A354**, 591 (1995)
19. J.F. Ziegler, J.P. Biersack and U. Littmark, The Stopping and Ranges of Ions in Matter, vol. 1 (Pergamon, London, 1985)
20. R. Wyss, W. Nazarewicz and A. Johnsson. Nucl. Phys. **A503**, 285 (1989)
21. S. Ćwiok *et al.*, Comp. Phys. Comm., **46**, 379 (1987)
22. W. Satula and R. Wyss, Phys. Script. **T56**, 159 (1995)
23. W. Satula, R. Wyss and P. Magierski, Nucl. Phys. **A578**, 45 (1994)
24. Y. Nogami, H.C. Pradhan and J. Law, Nucl. Phys. **A201**, 357 (1973)
25. F. Lerma *et al.*, submitted to Phys. Rev. Lett